J. Phys. G: Nucl. Phys., Vol. 4, No. 8, 1978. Printed in Great Britain

803

Measurement of the depolarisation factor $D(\theta)$ for the reaction $^2H(\vec{n}, \vec{n})^2H$ at 2·45 MeV†

D Bovet‡, P Chatelain, R Viennet and J Weber

University of Neuchâtel, Institute of Physics, Rue A-L Breguet 1, CH-2000 Neuchâtel, Switzerland

Received 28 November 1977, in final form 24 February 1978

Abstract. The angular distribution of the depolarisation factor $D(\theta)$ has been measured for the n–^{2}H scattering at 2·45 MeV. The incident polarised neutron beam was produced from the $^{12}C(d, \vec{n})^{13}N$ reaction at 25° lab. Two sets of phase-shifts between 0 and 3·27 MeV have been determined by fitting the cross sections in the frame of effective range approximation (ERA). We compare our experimental results with these phase-shift predictions.

NUCLEAR REACTIONS $^2H(\vec{n}, \vec{n})^2H$, $E = 2{\cdot}45$ MeV; measured depolarisation factor $D(\theta)$; comparison with ERA-analyses predictions.

1. Introduction

For a complete description of n–^{2}H scattering one has to know the scattering amplitudes for both the spin channel states $\frac{3}{2}$ (quartet channel) and $\frac{1}{2}$ (doublet channel). The quartet amplitudes are well determined experimentally as well as theoretically (Bovet *et al* 1973). The situation for the doublet amplitudes, which are the most interesting ones, is not clear and the measurements of observables sensitive to that quantity are highly desirable. The depolarisation factor $D(\theta)$ exhibits such a sensitivity (Jaccard and Viennet 1972). We therefore undertook measurements of the angular distribution of $D(\theta)$ below the deuteron break-up threshold at 2·45 MeV neutron energy.

The measurement of the $D(\theta)$ parameter requires a triple-scattering experiment in which the first scattering produces a polarised beam of neutrons and the third scattering measures the polarisation of the beam after it has been scattered at the second scatterer, all scatterings taking place in the same plane. The $D(\theta)$ parameter is a measure of the change in polarisation of the beam, perpendicular to the scattering plane, due to the scattering in the second target. If all the scattering planes are chosen parallel, the asymmetry ϵ is related to the depolarisation factor $D(\theta)$ by (Wolfenstein 1956)

$$\epsilon = \frac{P(\theta) + D(\theta)\boldsymbol{P}_1 \cdot \boldsymbol{n}_s}{1 + P(\theta)\boldsymbol{P}_1 \cdot \boldsymbol{n}_s} A$$

† Work supported in part by the Swiss National Science Foundation.
‡ This article includes parts of the PhD thesis of D Bovet.

where $P(\theta)$ is the polarisation for n–^{2}H scattering, A the analysing power, $\boldsymbol{P}_1$ the polarisation of the incident beam and $\boldsymbol{n}_s$ a unit vector perpendicular to the scattering planes.

2. Experimental set-up

Polarised neutrons were produced from the reaction $^{12}C(d, \vec{n})^{13}N$, with a resulting polarisation $\boldsymbol{P}_1 = -0{\cdot}45\ \boldsymbol{n}_s$ (Sawers *et al* 1968). They were then scattered by a deuterated scintillating detector (D1) composed of a C_6D_6 liquid. The polarisation of the scattered neutrons was determined by means of a polarimeter consisting of a liquid helium scatterer (D2) and two completely identical NE-102 plastic detectors ($D3_L$, $D3_R$), each being coupled through a light pipe to a common photomultiplier. A movable optical shutter was placed between each detector and the corresponding light pipe, so that asymmetry measurements were performed by alternative closing of the left and right shutters. This was controlled by the beam current integrator. A more detailed description of this system has been given by Piffaretti (1971). A schematic drawing of the experimental set-up is given in figure 1.

Spectroscopic information was obtained by recording the recoil energy spectra of detectors D1, D2 and D3, and the timing information given by time-of-flight spectra between D1 and D2 (TF12) and D2–$D3_L$ ($TF23_L$), D2–$D3_R$ ($TF23_R$). The numbers of neutrons scattered into $D3_L$ and $D3_R$ (called I_L and I_R respectively) were obtained by integrating $TF23_L$ and $TF23_R$ respectively. These events had to satisfy

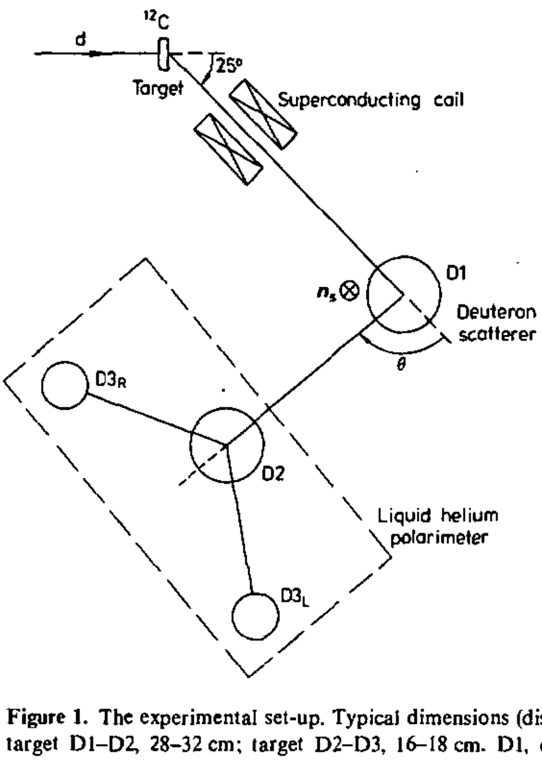

Figure 1. The experimental set-up. Typical dimensions (distances): target –D1, 35–40 cm; target D1–D2, 28–32 cm; target D2–D3, 16–18 cm. D1, cylinder ∅ 3 cm, height 3 cm; D2, sphere ∅ 5 cm; D3, cylinder ∅ 2·54 cm, height 3·8 cm.

some conditions imposed on the parameters defined above so that only neutrons corresponding to the correct triggers (D1–D2–$D3_L$ and D1–D2–$D3_R$) were taken into account. Asymmetry is then given by

$$\epsilon = \frac{I_R - I_L}{I_R + I_L}.$$

In order to eliminate false asymmetry, measurements were also performed with incoming neutrons of opposite polarisation, $-\boldsymbol{P}_1$. For this purpose, a superconducting coil magnet was used to change the sign of the incident polarisation. The true asymmetry is then given by (Piffaretti 1971)

$$\epsilon_t = \tfrac{1}{2}(\epsilon - \tilde{\epsilon})$$

where ϵ is the asymmetry without magnetic field (phase 1) and $\tilde{\epsilon}$ is the asymmetry with magnetic field (phase 2).

There are two main difficulties in this kind of experiment.

(i) The low counting rate inherent in a triple-scattering experiment; thus rather large, closely placed, detectors must be used to increase the counting rate. However, this kind of set-up leads to a high level of multiple-scattered events and other geometrical effects, which must be taken into account in a Monte-Carlo program, simulating the experiment completely. With typical dimensions like those given in figure 1, the counting rate for true events was only 6–10 h^{-1}.

(ii) The structure of the background; direct neutrons scattered from D2 to $D3_L$ or $D3_R$, together with a non-correlated event in D1, give rise to events which are not distinguishable from true events if only TF23 is considered. Shielding reduces these parasite events but the exact amount of this contamination can only be eliminated by careful examination of the correlated spectra TF12 with $TF23_L$ (and TF12–$TF23_R$).

3. Data recording

A block diagram of the electronics is given in figure 2. Spectroscopic information about the detectors D1, D2 and D3 was derived from dynode 14 and was fed through a linear gate and strecher module (LG) and then converted to digital information by means of an analogue to digital converter (ADC). This information was read by a fast scaler (FS). Timing information was obtained directly by sending the outputs of the anode to a time-to-digital converter (TDC). The start signal was provided by the detector D2, and two stop signals by the detectors D1 and D3 for the TF12 and TF23. A logic signal was used to indicate which one of the two shutters (left or right) was open. The fast coincidence units C2, C4 and C5 were used to select the events occuring in a given temporal sequence. Outputs from coincidences C1, C2 and C3 were used to gate the modules LG1, LG2 and LG3. Information from the TDC and FS modules was then sent to the PDP computer via a PDP–CAMAC interface which was built in our Institute. This module was activated by a signal derived from C2 (FE), and supplied a signal when the computer was busy (BL). Furthermore, the pile-up gate (PU) was used to inhibit the electronics and the beam current integrator for a fixed period (300 μs), thus eliminating the need for dead-time corrections.

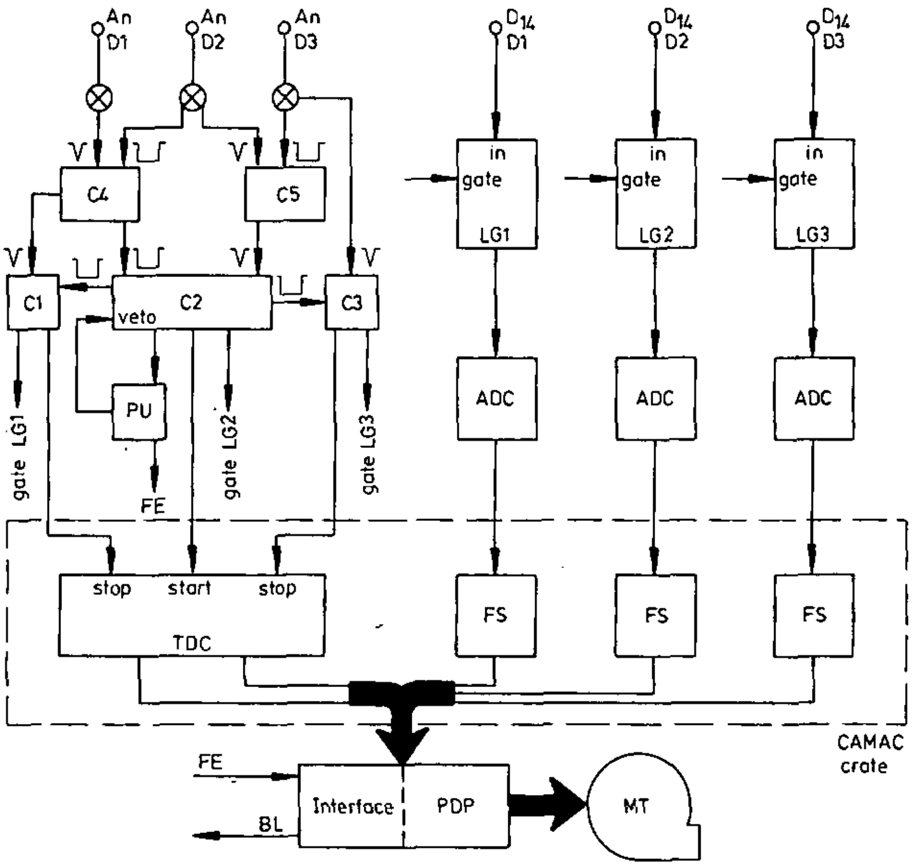

Figure 2. Block diagram of the electronics. An D1–D3, anode of detector D1, D2, D3; D_{14} D1–D3, 14th dynode of detector D1, D2, D3; C1–C5, fast coincidences; PU, pile-up gate generator; TDC, time to digital converter; LG1–LG3, linear gate and stretcher; ADC, analogue to digital converter; FS, fast scaler (40 Mc/s); ⊗, zero crossing module; MT, magnetic tape.

The five kinematical parameters (three recoil spectra and TF12, TF23) were recorded by the PDP computer and written on the magnetic tape (MT) together with the logic parameter indicating which shutter was open.

4. Background-subtracted spectra

Events were sorted out by an off-line treatment by imposing the kinematical conditions on the parameters. In particular, the correlated spectra TF12–$TF23_L$ and TF12–$TF23_R$ were established (see, for example, figure 3). From these, it was possible to study the structure of the background and subtract it. Asymmetry was extracted after integrating the time-of-flight peaks of the net spectra. The limits of the integration were chosen very carefully to have a reasonable stability for the asymmetry.

5. Monte-Carlo simulation program

The experimental situation was simulated completely by means of a program based on the Monte-Carlo method. We have assigned a certain weight to the scattered

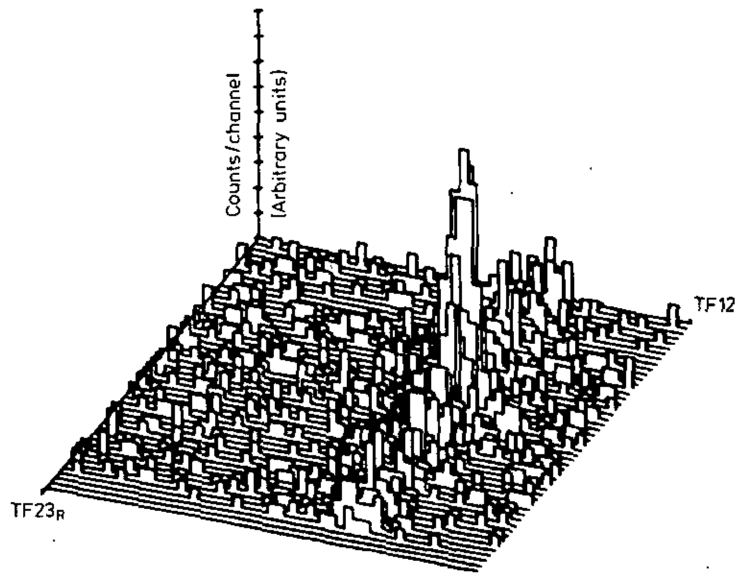

Figure 3. Example of a correlated time-of-flight spectrum.

neutron depending on its trajectory in the scatterers. For the detectors D1 and D2, three possible scatterings have been taken into account. The polarisation of the neutron was calculated after each scattering. The time-of-flight spectra $TF23_L$ and $TF23_R$ were constructed with the same kinematical constraints as in the experiment and from these the asymmetry was calculated. Each of the phases, with and without magnetic field, has been simulated independently giving the two asymmetries ϵ^s and $\overline{\epsilon^s}$. The combination $\epsilon_t^s = \frac{1}{2}(\epsilon^s - \overline{\epsilon^s})$ was then compared with the experimental value ϵ_t. The value of the unknown quantity $D(\theta)$ was adjusted by trial and error until ϵ_t^s was equal to the experimental value.

The simulation program requires a complete knowledge of n–^{12}C and n–^{4}He scattering below 3 MeV (in addition to n–^{2}H scattering). The corresponding cross sections and polarisation parameters have been calculated from phase-shifts given by Stammbach and Walter (1972) and Lane *et al* (1969).

The following approximations have been used in the program.

(i) Since n–^{2}H scattering is so far insufficiently known, the polarisation observables have been calculated in the frame of the diagonal, J-degenerated model, which predicts $P(\theta) = 0$ and the scattered neutron polarisation $= D(\theta)P_1$ (Jaccard and Viennet 1972). This model is thought to be sufficient for the present situation because the measured polarisation is small (Piffaretti 1971, Haeberli 1969) ($<5\%$) and the effect of $P(\theta) \neq 0$ will cancel at the first-order approximation when both phases (with and without magnetic field) are combined. Furthermore, $D(\theta)$ was set to a constant for all angles and energies.

(ii) The influence of detector D3 was taken into account by considering only its neutron detection efficiency.

(iii) The finite resolution of the electronics was taken into account by folding the simulated spectra with an adequate function of resolution.

Table 1. Measured depolarisation factor $D(\theta)$ for n–^{2}H scattering at 2·45 MeV. The errors quoted are statistical.

θ_{lab}(deg)	θ_{CM}(deg)	$\epsilon_1 \pm \sigma(\epsilon_1)$(%)	$D \pm \sigma(D)$
30	45	9 ± 4·4	0·31 ± 0·15
40·5	60	8·8 ± 4·4	0·34 ± 0·17
55	80	13·1 ± 4·0	0·54 ± 0·17
70	100	18·1 ± 4·0	0·66 ± 0·15

6. Results

To test the whole apparatus and simulation program, we first performed one measurement on hydrogen for which $D(\theta)$ was known. Our results are in satisfactory agreement with the predictions of the effective range theory (Noyes 1972).

Our measured values of $D(\theta)$ for n–^{2}H scattering at 2·45 MeV are presented in table 1. They are also shown in figure 4 together with theoretical calculations by Kloet and Tjon (1973, local S-wave N–N interaction), Sloan (1971, separable S wave) and the Lyon group† (Fayard 1976, private communication, separable S, P and $^3S_1$–$^3D_1$ waves).

7. Phase-shift analysis

A phase-shift analysis between 0 and 3·27 MeV has also been undertaken; this showed the importance of $D(\theta)$ measurements.

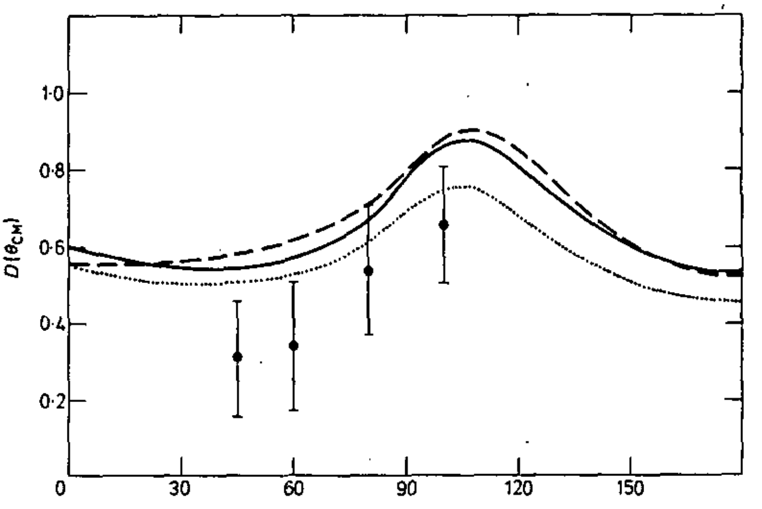

Figure 4. Measurements and calculations of $D(\theta)$. Data points, our measurements at 2·54 MeV; dotted curve, calculation by Sloan (1971) at 2·45 MeV; full curve, calculation by Kloet and Tjon (1973) at 2·45 MeV; broken curve, calculation by the Lyon group at 2·6 MeV (Fayard 1976, private communication).

† The authors are grateful to the Lyon group, particularly to C Fayard, for supplying the results of their calculations prior to publication.

A smooth energy dependence was imposed on the phases through the ERA approximation. (This allows as many measurements as possible to be taken into account at the same time.) In order to reduce the number of free parameters we have performed our analysis in the frame of the diagonal, J-degenerated model (which implies that we have degenerated phase-shifts and no mixing parameters; see Jaccard and Viennet (1972) and Viennet (1972)), and we have limited the l values to $l \leqslant 2$. The following measurements were included in our analysis:

(i) 38 measurements of σ_{tot} (quoted in Viennet 1972);

(ii) 38 measurements of $\sigma(\theta)$ (quoted in Viennet 1972);

(iii) 4 measurements at zero energy (σ_0, $a_4 + \frac{1}{2}a_2$, a_4, a_2) (Dilg *et al* 1971, Nikitin *et al* 1956);

(iv) the binding energy of the triton (quoted in Viennet 1972).

The reader is reminded that, in the frame of our model, the polarisation parameter is identically equal to zero (Jaccard and Viennet 1972). Therefore no such experimental results have been included in our analysis.

Two types of parametrisation have been used:

Set I

$$k^{2l+1} \cot \delta_{ls} = A_{ls} + \tfrac{1}{2}R_{ls}k^2 + P_{ls}k^4$$

for all phase shifts;

Set II

$$k \cot \delta_{0\frac{1}{2}} = A_{0\frac{1}{2}} + \tfrac{1}{2}R_{0\frac{1}{2}}k^2 + P_{0\frac{1}{2}}/(1 + k^2/W^2)$$

for the ^{2}S phase (Van Oers and Seagrave 1967), the parametrisation for the other phase-shifts being the same as for set I†. k is the centre-of-mass momentum, and A_{ls}, R_{ls}, P_{ls}, W are the parameters to be adjusted.

Both sets give equally good fits to the data. The values of the parameters are given in table 2. As far as the quartet phase-shifts are concerned, these two sets are completely equivalent and compatible with other published results (Seagrave 1969,

Table 2. Results of the two ERA analyses (see text).

	^{2}S	^{4}S	^{2}P	^{4}P	^{2}D	^{4}D
Set I: $\chi^2 = 98$; reduced $\chi^2 = 1.46$						
A_{ls}	-1.533	-1.576×10^{-1}	1.720	3.835×10^{-3}	9.169×10^{-4}	-4.405×10^{-4}
R_{ls}	-5.243×10^1	2.969	-1.273×10^2	9.355×10^{-1}	0	0
P_{ls}	-1.034×10^2	—	6.137×10^2	—	1.113	-2.550
Set II: $\chi^2 = 110$; reduced $\chi^2 = 1.72$						
A_{ls}	-2.265×10^{-1}	-1.576×10^{-1}	-1.478	1.988×10^{-3}	-2.727×10^{-2}	-3.134×10^{-3}
R_{ls}	2.727	2.885	1.053×10^2	1.254	6.329×10^{-1}	3.787×10^{-1}
P_{ls}	-1.315	—	-4.890×10^2	—	-8.544×10^{-1}	-4.813
W	8.780×10^{-2}	—	—	—	—	—

† Another parametrisation has been used by Phillips and Barton (1969).

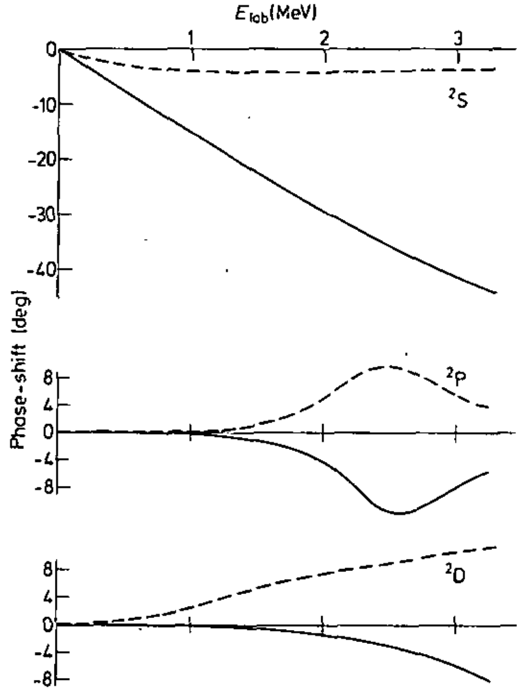

Figure 5. Doublet phase-shifts: results of ERA analysis. Broken curves, set I; full curves, set II.

Arvieux 1974). On the other hand, the doublet phase-shifts are completely different (figure 5). Set I has a ^{2}S phase much smaller than that of set II. ^{2}P phases are of opposite sign for the two sets. The ^{2}D phase of set I is much bigger than that of set II. Set II is closer to standard results except for the ^{2}D phase which has the opposite sign from that generally accepted.

The depolarisation factor $D(\theta)$, calculated with the phase-shifts from sets I and II, shows a completely different shape (see figure 6), indicating the sensitivity of this observable to the doublet amplitudes. Our experimental values of $D(\theta)$, which were not included in the ERA analysis, are also shown in figure 6. A visual inspection of this figure seems to indicate that the trend is in favour of set II. The appearance of the pole in the parametrisation of the ^{2}S phase-shift has been shown by exact three-body calculations (see, for example, Whiting and Fuda 1976).

Finally, we would like to point out that the results of the present ERA analysis could be used as a satisfactory starting point for an analysis which would include mixing parameters and/or split phase-shifts. This analysis could be used for fitting polarisation data (Bovet *et al* 1976).

8. Conclusion

The present experiment shows that triple-scattering experiments with neutrons are feasible, though difficult.

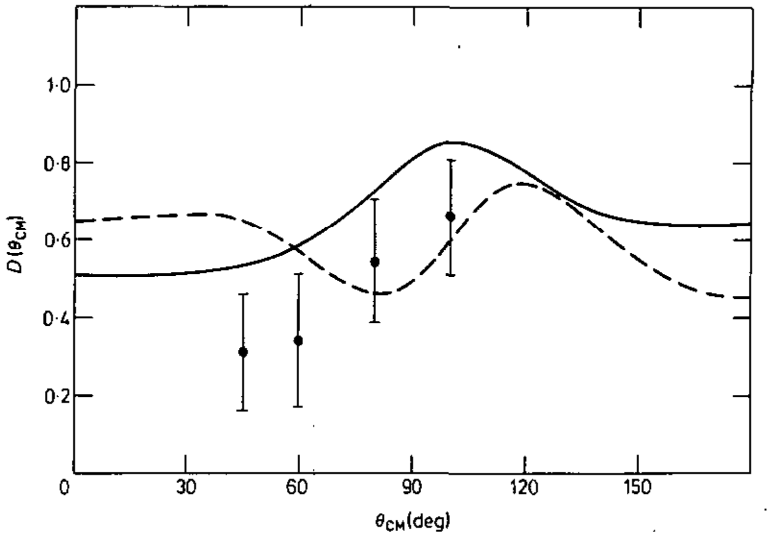

Figure 6. Depolarisation at 2·45 MeV. Measurements and results of ERA analysis. Broken curve, set I; full curve, set II; data points, our measurements.

$D(\theta)$ is an observable sensitive to the less well known doublet amplitudes and the measurement of that quantity should give some useful information in determining the n–^{2}H scattering matrix.

The disagreement between experimental values and the theoretical 'exact' predictions still requires clarification.

Acknowledgments

We are grateful to the Institute of Physics of Zürich University for the fabrication of the C targets. We should also like to thank the computer centres of the University of Neuchâtel and EPF–Lausanne for providing many hours of computer time.

References

Arvieux J 1974 *Nucl. Phys.* A **221** 253

Bovet D, Chatelain P, Jaccard S, Onel Y, Piffaretti J, Viennet R and Weber J 1976 *Proc. Int. Conf. on the Interactions of Neutrons with Nuclei* ed E Sheldon p 1357

Bovet D, Jaccard S and Weber J 1973 *Helv. Phys. Acta* **46** 668

Dilg W, Koester L and Nistler W 1971 *Phys. Lett.* **36B** 208

Nikitin S J, Smolyankin W T, Kolganow W Z, Lebedev A W and Lomkaży G S 1956 *The First International Conference on Peaceful Uses of Atomic Energy (Geneva 1955)* (New York: United Nations) vol 2 p 81

Haeberli W 1969 *Proc. 1st Int. Conf. on the Three-Body Problem, Birmingham* eds J S C McKee and P M Rolph

Jaccard S and Viennet R 1972 *Nucl. Phys.* A **182** 541

Kloet W M and Tjon J A 1973 *Ann. Phys., NY* **79** 407

Lane R O, Koshel R D and Monahan J E 1969 *Phys. Rev.* **188** 1618

Noyes H P 1972 *Ann. Rev. Nucl. Sci.* **12** 717

Phillips A C and Barton G 1969 *Phys. Lett.* **28B** 378

Piffaretti J 1971 *Helv. Phys. Acta* **44** 763
Sawers J R, Morgan G L, Schaller L A and Walter R L 1968 *Phys. Rev.* **168** 1102
Seagrave J D 1969 *Proc. 1st Int. Conf. on the Three-Body Problem, Birmingham* eds J S C McKee and P M Rolph
Sloan I H 1971 *Nucl. Phys.* A **168** 211
Stammbach Th and Walter R L 1972 *Nucl. Phys.* A **180** 225
Van Oers W T H and Seagrave J D 1967 *Phys. Lett.* **24B** 562
Viennet R 1972 *Nucl. Phys.* A **189** 424
Whitting J S and Fuda M G 1976 *Phys. Rev.* C **14** 18
Wolfenstein L 1956 *Ann. Rev. Nucl. Sci.* **6** 43